

## CHAPTER VII

# ANALYSIS OF ENCAPSULATION POTENCY OF $\alpha$ - AND $\beta$ - CYCLODEXTRIN TO 4-CHLORO-1-NAPHTHOL IN AQUEOUS ETHANOL MEDIA

---

### Abstract

The present work deals with the formation and investigation of host-guest inclusion complexes of 4-chloro-1-naphthol insight into  $\alpha$ - and  $\beta$ -cyclodextrin in 50% aqueous ethanol media by various physicochemical and spectroscopic methods. Job's plots have been drawn by UV-visible spectra and confirm 1:1 stoichiometry of the complex. Surface tension data also support 1:1 stoichiometry of the complexes.  $^1\text{H}$  NMR, FTIR and ESI MS studies ensure the inclusion phenomenon once again. Association constants have been calculated by UV-Visible spectroscopy on the basis of the Benesi-Hildebrand method and non-linear programme, and the thermodynamic parameters have been estimated with the help of Van't Hoff equation. The higher binding constant values and calculated values of thermodynamic parameters such as Gibb's free energy, enthalpy and entropy supported the high stability and feasibility of formation of the inclusion complex. The formations of inclusions have been elucidated by H-bonding interactions, hydrophobic effects, structural effects, and electrostatic interaction.

**Keywords:** 4-chloro-1-naphthol;  $\alpha$ -cyclodextrin;  $\beta$ -cyclodextrin; Inclusion complex; Surface tension and spectroscopic study

## 1. Introduction

Cyclodextrins (CDs) are doughnut-shaped cyclic oligosaccharides consist of D-glucopyranose units connected by  $\alpha$ -(1,4) linkages. [1] There are some types of cyclodextrins, commons amongst are having six, seven, and eight D-glucopyranose units and are known as  $\alpha$ -,  $\beta$ -, and  $\gamma$ -CDs, respectively. [2,3] Due to the presence of cavity of hydrophobic nature, CDs show a phenomenal property of accommodating hydrophobic part of guest molecules into its cavity to form inclusion complexes (ICs). [4] The hydroxyl groups present at the wider and narrow rim of CD act as stabilizer through H-bond with the hydrophilic part of guest molecules. [2] The macromolecule remarkably shields the embedded guest molecules from degradation by auto-oxidation, hydrolysis, proteolysis in the solid state. [1] The encapsulation and controlled release properties of CD have been excellently applied in medicine as drug delivery system. CD can also increase the solubility of the guest in industrial purposes, food department, customization of cosmetic, paint industry, elimination of various toxic materials, pollutants, and waste products without a chemical change. [5]

One of the  $\alpha$ -naphthol derivatives, 4-chloro-1-naphthol (4C1N) (Scheme VII.1) is primarily used for the detection of protein, Scanning Electrochemical Microscopy (SEM), and for imaging of DNA hybridization on microscopic polypyrrole patterns. It can also be used as a substitute for benzidine compounds, which are considered to be carcinogenic. Therefore, the encapsulation and controlled release of 4-chloro-1-naphthol without chemical and biological distortion, may give a new direction of its application.

For this, in the present study we have investigated the nature of formation and stoichiometry of inclusion complex of  $\alpha$ -CD and  $\beta$ -CD with 4-chloro-1-naphthol in aqueous ethanolic media. Interactions between the 4-chloro-1-naphthol and CDs have been analyzed in terms of surface tension and spectroscopic study viz., UV-Vis,  $^1\text{H}$  NMR, FTIR, and HR MS.

## 2. Experimental section

### 2.1. Materials

4-Chloro-1-naphthol,  $\alpha$ - and  $\beta$ -cyclodextrin of puris grade of purity  $\geq 98.0\%$ , were purchased from Sigma-Aldrich and have been used without further purification. Triple distilled water having the conductance  $1 \cdot 10^{-6} \text{ S} \cdot \text{m}^{-1}$  has been used to prepare the solutions.

### 2.2. Apparatus

UV-visible spectra were recorded using a JASCO V-530 UV-VIS spectrophotometer having a wavelength accuracy of  $\pm 0.5 \text{ nm}$ . A digital thermostat was used to maintain the cell constant and temperature.

Surface tension has been measured using platinum ring detachment technique with a K9 digital tensiometer (Krüss GmbH, Hamburg, Germany) at the experimental temperature, with an accuracy of  $\pm 0.1 \text{ mN} \cdot \text{m}^{-1}$ . Temperature has been maintained by the circulation of auto thermostat water through a double-walled glass vessel containing the solution.

$^1\text{H}$  NMR spectra has been recorded in DMSO using Bruker Avance 400 MHz instrument. Signals have been cited as  $\delta$  values in ppm with reference to residual protonated solvent signal as the internal standard (HDMSO,  $\delta$  2.50 ppm). Data are presented as chemical shifts.

FTIR spectra were recorded by means of Perkin-Elmer FTIR spectrometer using KBr disk method within the range of  $4000\text{--}500 \text{ cm}^{-1}$  at room temperature.

Using JEOL JSM-IT 100 Scanning Electron Microscope (SEM), the surface morphologies of 4C1N, CDs and both of the inclusion complexes were recorded. The pictures were taken at an excitation voltage of 15, 20 and 30kV with a magnification of 425, 500, 1000 and 2000X.

HRMS spectra of the solid ICs were measured by using Quadrupole Time-Of-Flight (Q-TOF) high resolution instrument with positive-mode electrospray ionization. Methanol solutions of the solid ICs were employed for such spectral measurement.

### 2.3. Procedure

Before executing the practical experiments, the solubility of host and both the guest molecules have been thoroughly checked. While,  $\alpha$ -,  $\beta$ -cyclodextrins were quite soluble in water, 4-chloro-1-naphthol was only poorly soluble in water. Then the solubility of all the compounds were examined in aqueous ethanol (v:v=1:1) solvent. Both the CDs and the guest showed a marked increase in solubility in this mixed solvent. Hence, all the solutions were prepared by adding known volume of aqueous ethanol in air tight stoppered bottle. The mass measurements were accomplished by using a Mettler Toledo AG-285 electronic balance with an uncertainty of  $\pm 0.1$  mg at 298.15 K. Precautions were taken to minimize weight loss due to evaporation while mixing and working with the solutions.

In order to prepare the solid inclusion complexes, 20 ml (1.0 mM) solutions of each,  $\alpha$ - and  $\beta$ -cyclodextrins were prepared separately and stirred continuously for approximately 6 hours using a magnetic stirrer. Thereafter, 20 ml (1.0 mM) solutions of 4C1N were added dropwise separately to the previously made guest solutions so as to make the ultimate equimolar mixtures, which were allowed to continuous stir for almost 48 hours, keeping the temperature 55-60 °C. The resultant suspensions were cooled to 5 °C and then filtered to obtain white and crystalline powders. These were then dried in air and finally, kept in a desiccator for further experimental use.

## 3. Results and discussion

### 3.1. Tensiometric Study

Surface tension ( $\gamma$ ) provides strong testimony about the inclusion phenomenon and also the stoichiometry of the inclusion complexes formed. [6] The values of surface tension of the 4C1N solutions were determined with gradual addition of CDs at 298.15K (Figure VII.1). In both the cases ( $\alpha$ -CD and  $\beta$ -CD), the  $\gamma$ -values were increasing with increasing

the concentration of the hosts. [7,8] These trends are probably due to the insertion of 4C1N molecule into the cavity of CDs from the bulk, forming inclusion complexes. [9] But, the remarkable observation was found at a definite concentration of CD, where, a sudden break point obtained. Moreover, after the break point, the curve remains almost flattened, even after further addition of CD. This inflection point indicates the saturation of inclusion and from this point we can determine the probable stoichiometry of the complex formed. The break points around the concentration of 5mM of the CDs (where the concentration of 4C1N solutions were taken 5mM) implies 1:1 stoichiometry for both the complexes. [10,11]

### 3.2. Continuous Variation Method

The stoichiometry of the host-guest inclusion complexes can also be predicted by Job's method or continuous variation method. [12] The method has been employed by making use of UV-visible spectroscopy. Initially, 100 $\mu$ M solutions of 4C1N,  $\alpha$ -CD and  $\beta$ -CD were prepared separately. Then (4C1N+  $\alpha$ -CD), and (4C1N+  $\beta$ -CD) solutions were prepared separately by varying the molar ratio viz., 4ml:0ml, 3.6ml:0.4ml, 3.2ml:0.8ml and so on with keeping the total concentration of species constant. After that, absorbance at  $\lambda_{\max}$  was determined at 298.15K. Then Job plots were obtained by plotting  $\Delta A \times R$  against  $R$ , (Figure VII.2.) (where  $\Delta A$  is the difference in absorbance of 4-chloro-1-naphthol without and with of cyclodextrins, and  $R = \frac{[4C1N]}{[4C1N]+[CD]}$ ). [13,14] This ratio ( $R$ ) gives rise to the stoichiometry of the inclusion complexes. For instance, if  $R=0.33$ , 0.50, & 0.67, the ratio of the guest and host in the complexes are 1:2, 1:1, & 2:1 respectively. In Figure VII.2, maxima of plot for each solution was found at  $R=0.5$ , which reveals the 1:1 stoichiometry for both the inclusion complexes.

### 3.3. Association constant and other thermodynamic parameters

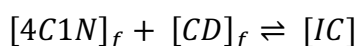
The extent of encapsulation of the guest into the cavity of the hosts as also the stability of the inclusion complexes thus formed were explored by estimating the association constants ( $K_a$ ) of both the ICs. The association power in terms of constant ( $K_a$ ) for the ICs has been determined by means of UV-Vis spectroscopic study. [15] Benesi-Hildebrand method has been used to quantify the association constant for the 1:1 host-

guest inclusion compound, the double reciprocal plot has been obtained using the following equation [1,14,16,17],

$$\frac{1}{\Delta A} = \frac{1}{\Delta \epsilon [4C1N] K_a [CD]} + \frac{1}{\Delta \epsilon [4C1N]}$$

Where,  $\Delta A$  represent the difference in absorbances of 4C1N before and after complexation with CDs. Depending upon the solvent polarity, the molar extinction coefficient ( $\Delta \epsilon$ ) of 4C1N should change on going from polar aqueous ethanolic media to the apolar hydrophobic cavity of the cyclodextrins to form the inclusion complexes. [16,18] In order to determine the association constant ( $K_a$ ), changes in absorbance values ( $\Delta A$ ) of 4C1N were measured with increasing concentration of CDs at various temperatures viz., 298.15K, 303.15K and 308.15K (Table S1, S2, supporting information). For 4C1N,  $\lambda_{\max} = 211\text{nm}$  was considered to calculate the association constant ( $K_a$ ), which has been obtained by dividing the slope by the intercept of the plot and the values have been listed in Table VII.1. The magnitudes of  $K_a$  indicate that complexes are formed with strong association between host and guest molecules.

Fitting UV-Vis spectral data in a non-linear program, the changes in absorbance of 4C1N owing to its recognition into the apolar cavities of cyclodextrins and the association constants ( $K_a^\theta$ ) were obtained. [1,10,19] The following equilibrium was expected to exist between the guest, host and 1:1 inclusion complex. [20,21]



Thus,

$$K_a^\theta = \frac{[IC]}{[4C1N]_f [CD]_f}$$

Where,  $[IC]$ ,  $[4C1N]_f$  and  $[CD]_f$  are the equilibrium concentration of inclusion complex, free 4C1N and cyclodextrins respectively.  $K_a^\theta$  in terms of absorbance, can be expressed as,

$$K_a^\theta = \frac{[IC]}{[4C1N]_f [CD]_f} = \frac{(A_{obs} - A_0)}{(A - A_{obs}) [CD]_f}$$

Here,

$$[4C1N]_x = [CD]_x - \frac{[4C1N]_x (A_{obs} - A_0)}{(A - A_{obs})}$$

Where,  $A_0$  is the absorbance of 4C1N molecules in the initial state,  $A_{obs}$  stands for the absorbances of the same during the gradual addition of cyclodextrins and  $A$  denotes the final concentration of 4C1N molecules.

$[4C1N]_x$  and  $[CD]_x$  are respectively the concentrations of guest and CDs added. Resulting  $K_a^\theta$  values from binding isotherm applying non-linear program were listed in Table 2. Thermodynamic properties like standard enthalpy ( $\Delta H^0$ ), standard entropy ( $\Delta S^0$ ), and free energy ( $\Delta G^0$ ) also predicting the feasibility of complexation. The lower  $\Delta G^0$  value for IC2 than for IC1, indicate a better fitting of the guest insight into the cavity of  $\beta$ -CD than that of  $\alpha$ -CD by non-covalent bond like electrostatic attraction, van der Waal force, hydrogen bond or hydrophobic interactions.

### 3.4. $^1\text{H}$ NMR spectral analysis of solid inclusion complexes

The molecular encapsulation has also been studied with the help of  $^1\text{H}$ NMR spectroscopy. The insertion of a guest into the cavity of the CDs is certainly associated with a change in the chemical shift values of the interacting protons of both the compounds, because of their mutual shielding through space. [20,21] The protons in CDs are held in different environments. H3 and H5 protons are situated inside the conical cavity; also we notice that H3 proton is located near the wider rim and H5 proton nearer to the narrower rim. The other protons viz., H1,H2 and H4 were oriented at the exterior of the CD molecule (Scheme VII.2). [12,22]  $^1\text{H}$  NMR spectra of pure 4C1N, pure CDs and the inclusion complexes are included in Figures VII.3 and VII.4. The signals of the interior H3 and H5 hydrogens of CDs as well as the interacting aromatic protons of 4C1N showed considerable up-field shifts (Tables VII.3 & VII.4), confirming the generation of inclusion complexes. [13] [23] The higher chemical shift ( $\delta$ ) of the H3 proton than that of the H5 proton, also signify that the guest probably entered through the wider rim of  $\alpha$ - and  $\beta$ -CD (Scheme VII.3). [24]

### 3.5. FTIR spectroscopy

The authenticity about the way the inclusion complexes are formed can be revealed by interpreting the IR spectroscopic data of the pure guest, pure host, and the inclusion complexes. Changes observed in the significant peak values while going from pure guest

or host molecules to the complex (Figure VII.5 and VII.6) suggests the formation of inclusion complexes with the binding between the 4C1N and the CDs. [23,25]

#### **FTIR spectra of the IC1 along with the spectra of pure $\alpha$ -CD and 4C1N:**

-O-H stretching frequency of  $\alpha$ -CD and the -O-H and aromatic -C-H stretching frequencies of 4C1N were observed at 3398, 3413 and 3232  $\text{cm}^{-1}$  respectively, which appears as a broad peak at 3431  $\text{cm}^{-1}$  in case of the IC1. The responsible fact for this shifting in frequencies is the formation of H-bond between 4C1N and  $\alpha$ -CD.

The peaks at 1052  $\text{cm}^{-1}$  responsible for the -C-O stretching for phenolic -C-OH group of 4C1N is shifted to 1027  $\text{cm}^{-1}$  correspondingly for the IC1. Thus, weakening of -C-O bond proposes the formation of H-bond with the H-3 of  $\alpha$ -CD via the phenolic -OH group of the guest molecule.

The stretching and bending frequencies for the -C-H bond of the  $\alpha$ -CD was at 2926 $\text{cm}^{-1}$  and 1414  $\text{cm}^{-1}$  and -C-H the out-of-plane bending frequency for 4C1N were at 753 $\text{cm}^{-1}$ . But in case of IC1, their existence is observed at 2922, 1343, 750 $\text{cm}^{-1}$  (very weak), suggesting that the interactions must be taking place between 4C1N and  $\alpha$ -CD (Figure 5).

#### **FTIR spectra of the IC2 along with the spectra of pure $\alpha$ -CD and 4C1N:**

The signal for -O-H stretching of  $\beta$ -CD was at 3392  $\text{cm}^{-1}$  and the -O-H and aromatic -C-H stretching frequencies of 4C1N were at 3413 $\text{cm}^{-1}$  and 3232 $\text{cm}^{-1}$  respectively, whereas, in the IC these signals shifted to 3433 $\text{cm}^{-1}$  correspondingly. This is possibly due to the formation of H-bonding between 4C1N and  $\beta$ -CD.

The peaks for -C-O (phenolic -C-OH group) were at 1052 $\text{cm}^{-1}$ , which shifted to 1028 $\text{cm}^{-1}$ . This is probably owing to the formation of H-bond between 4C1N and  $\beta$ -CD.

The signals at 2926 $\text{cm}^{-1}$  and 1410 $\text{cm}^{-1}$  corresponding to -C-H stretching and -C-H bending of  $\beta$ -CD, almost disappeared in the IC2. This is indicative of extensive inclusion between the host and the guest molecule. On the other hand, -C-H out-of-plane bending for 4C1N molecule at 753 $\text{cm}^{-1}$ , is absent in the inclusion complex. The strong peak at 806 $\text{cm}^{-1}$  due to the C-Cl stretching for the guest molecule is also disappeared in the



complex. This may be because of the various interactions taking place while forming the supramolecular assembly between 4C1N and  $\beta$ -CD (Figure VII.6).

These observations further indicate that, 4C1N undergo more feasible inclusion with  $\beta$ -CD in comparison with  $\alpha$ -CD.

### 3.6. High Resolution Mass Spectrometric (HRMS) Analysis

The solid ICs were further analyzed by High Resolution Mass Spectrometry, by dissolving the complexes in methanol. The spectra were shown in Figure VII.7 and VII.8, and the observed peaks were listed into Table VII.5 with possible ions. The peaks at  $m/z$  1152.65 and 1174.12 correspond to  $[4C1N + \alpha\text{-CD} + H]^+$  and  $[4C1N + \alpha\text{-CD} + Na]^+$ , respectively. And the peaks at  $m/z$  1314.89 and 1336.76 correspond to  $[4C1N + \beta\text{-CD} + H]^+$  and  $[4C1N + \beta\text{-CD} + Na]^+$ , respectively. The spectra confirm the desired complexes, 4C1N +  $\alpha$ -CD and 4C1N +  $\beta$ -CD, were formed in the solid state with the 1:1 stoichiometric ratio 1:1. [26-28]

### 3.7. SEM

Like other high resolution microscopic techniques, Scanning Electron Microscopy (SEM) is another qualitative way to analyze the surface texture and particle size of solid materials.[16][29,30] The surface morphological structures of pure 4C1N,  $\alpha$ -CD,  $\beta$ -CD along with those of IC1 and IC2 are shown in Figure VII.9. Vast differences observed between the morphological structures of pure 4C1N or CDs and ICs. So, this is one of the evidences indicating the strong complexation.

### 3.8. Influence of host and guest structure

The two main factors determining the effectiveness of inclusion complex formations are (1) size of the guest molecule and (2) cavity diameter of the host molecule. The diameter of the cavity in  $\beta$ -CD is 6.0–6.5 Å, the same in the case of  $\alpha$ -CD is 4.7–5.3 Å. [7] By virtue of the presence of hydrophobic cavity and hydrophilic rims, cyclodextrin provide a fruitful environment for encapsulation. Non-polar part of a guest resides inside the cavity and the polar part gets associated with the polar rims, thereby resulting in the stabilization of the whole inclusion compound. [2] Some water

molecules are present into the cavity of cyclodextrin. Their expulsion from the hydrophobic cavity into the bulk is the main driving force.[31] The hydrophobic part of the guest is pulled insight into the cavity so as to form the strong host-guest complex and the overall process is energetically favorable.[32] However, no covalent bond is broken or formed during the process of formation of inclusion complex.[33] The insertion of a 4C1N molecule into the cavity of a cyclodextrin molecule is expected to take place from the wider rim, to make utmost contact of the aromatic moiety with the cyclodextrin cavity.[7] The -Cl and -OH group of 4C1N are projected outside the larger rim of CD in polar environment and can make H-bonds with the -OH groups at the rims of CD molecules and stabilize the complex (Scheme VII.3).

The IC is of 1:1 stoichiometry probably because of the intricacy for a second 4C1N molecule to be introduced into the cavity of CD followed by the first inclusion.

## 4. Conclusion

Characterization of solid state crystal using UV-VIS, FTIR, HRMS,  $^1\text{H}$  NMR spectroscopy, and the observed SEM pictures strongly support the formation of stable inclusion complexes. Association constant values obtained from UV-Vis spectroscopic study suggests that both the complexes are formed with strong binding affinity. Evaluation of Job plots and surface tension data shows that in both the cases 1:1 stoichiometric complexes are formed. One of the driving forces for the formation of the inclusion complex is the extrication of the water molecules from the hydrophobic cavity of cyclodextrin to the bulk, leading to an increase in the entropy of the system with a simultaneous decrease in Gibbs free energy. In NMR spectra, the chemical shift corresponding to H5 and H3 protons support that the incorporation occur from wider rim of cyclodextrin. More negative  $\Delta G^0$  value and more shifts in various IR stretching frequencies in case of complexation with  $\beta$ -CD indicate that IC2 is formed more feasibly than IC1. This is further supported by higher shifting of H3 and H5 protons in  $^1\text{H}$  NMR spectra for IC2. The bonds to form the ICs thus can be attributed in terms of hydrophobic, H-bonding interactions and other non-covalent interactions.

## **Acknowledgments**

Prof. M.N. Roy is immensely thankful to the UGC, New Delhi, Government of India, for being awarded One Time Grant under Basic Scientific Research via the grant-in-Aid no. F.4-10/2010 (BSR). One of the author (N. Roy) is highly thankful to the “State Fellowship” bearing reference No. 1743/R-2017 dated 18.04.2017 and UGC-SAP DRS-III, New Delhi (no. 540/6/ DRS/2007, SAP-1) for providing instrumental facilities. We also appreciate Mr. G. Sarkar, HOD., USIC, University of North Bengal, for executing SEM picture.

## **Conflicts of Interest**

All the authors declare that there are no conflicts of interest.

## TABLES

■ **Table VII.1.** Association Constants of 4C1N+ $\alpha$ -CD and 4C1N+ $\beta$ -CD complexes

System	Temperature /K	Slope $\times 10^4$	Intercept	Association constant ( $K_a$ )/M <sup>-1</sup>
4C1N+ $\alpha$ -CD	293.15	9.11	5.40	5930.74
	298.15	9.54	4.03	4227.01
	303.15	13.10	3.13	2399.99
4C1N+ $\beta$ -CD	293.15	9.24	6.42	6950.53
	298.15	10.60	5.20	4902.76
	303.15	14.70	4.48	3047.21

■ **Table VII.2.** Thermodynamic parameters of 4C1N+ $\alpha$ -CD and 4C1N+ $\beta$ -CD

System	Temperature /K	$K_a$ /M <sup>-1</sup>	$\Delta H^0$ /kJ mol <sup>-1</sup>	$\Delta S^0$ /J mol <sup>-1</sup> K <sup>-1</sup>	$\Delta G^0$ /kJ mol <sup>-1</sup>
4C1N+ $\alpha$ -CD	293.15	5927.55			
	298.15	4224.31	49.34	0.24	-20.50
	303.15	2390.79			
4C1N+ $\beta$ -CD	293.15	6950.53			
	298.15	4902.76	40.30	0.20	-21.54
	303.15	3047.21			

■ **Table VII.3.** Chemical shifts ( $\delta$ /ppm) of protons of cyclodextrins after complex formation

Protons	$\delta$ in $\alpha$ -CD	$\delta$ ( $\alpha$ -CD+4C1N)	$\Delta\delta$ ( $\alpha$ -CD+4C1N)	$\delta$ $\beta$ -CD	$\delta$ ( $\beta$ -CD+4C1N)	$\Delta\delta$ ( $\beta$ -CD+4C1N)
H3	3.63	3.59	0.04	3.77	3.57	0.20
H5	3.53	3.51	0.02	3.63	3.47	0.16

■ **Table VII.4.** Chemical shifts ( $\delta$ /ppm) of protons of 4C1N after complex formation

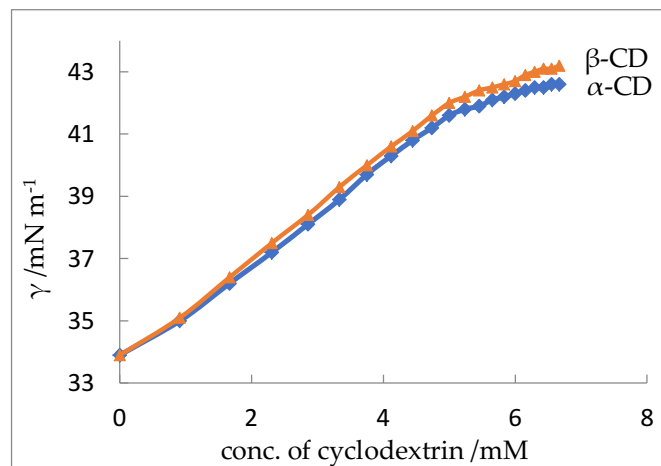
Protons	$\delta$ in 4C1N	$\delta$	$\Delta\delta$	$\delta$	$\Delta\delta$
		( $\alpha$ -CD+4C1N)	( $\alpha$ -CD+4C1N)	( $\beta$ -CD+4C1N)	( $\beta$ -CD+4C1N)
H2	6.85	6.83	0.02	6.69	0.16
H3	7.46	7.44	0.02	7.30	0.16
H5	8.18	8.16	0.02	8.03	0.15
H6	7.56	7.53	0.03	7.40	0.16
H7	7.66	7.63	0.03	7.50	0.16
H8	8.06	8.03	0.03	7.89	0.17

■ **Table VII.5.** Mass spectral data

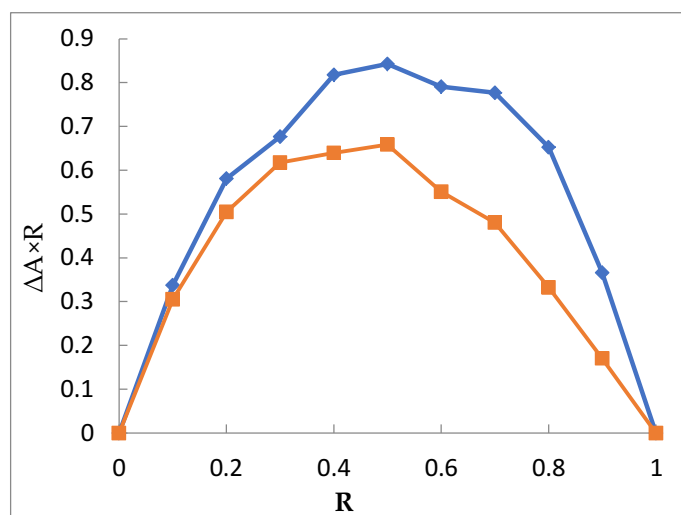
Name of the complexes	Calculated mass	Experimental mass
[4CN+ $\alpha$ CD+H] <sup>+</sup>	1152.45	1152.65
[4CN+ $\alpha$ CD+Na] <sup>+</sup>	1174.45	1174.12
[4CN+ $\beta$ CD+H] <sup>+</sup>	1314.59	1314.89
[4CN+ $\beta$ CD+Na] <sup>+</sup>	1336.59	1336.76

**FIGURES**

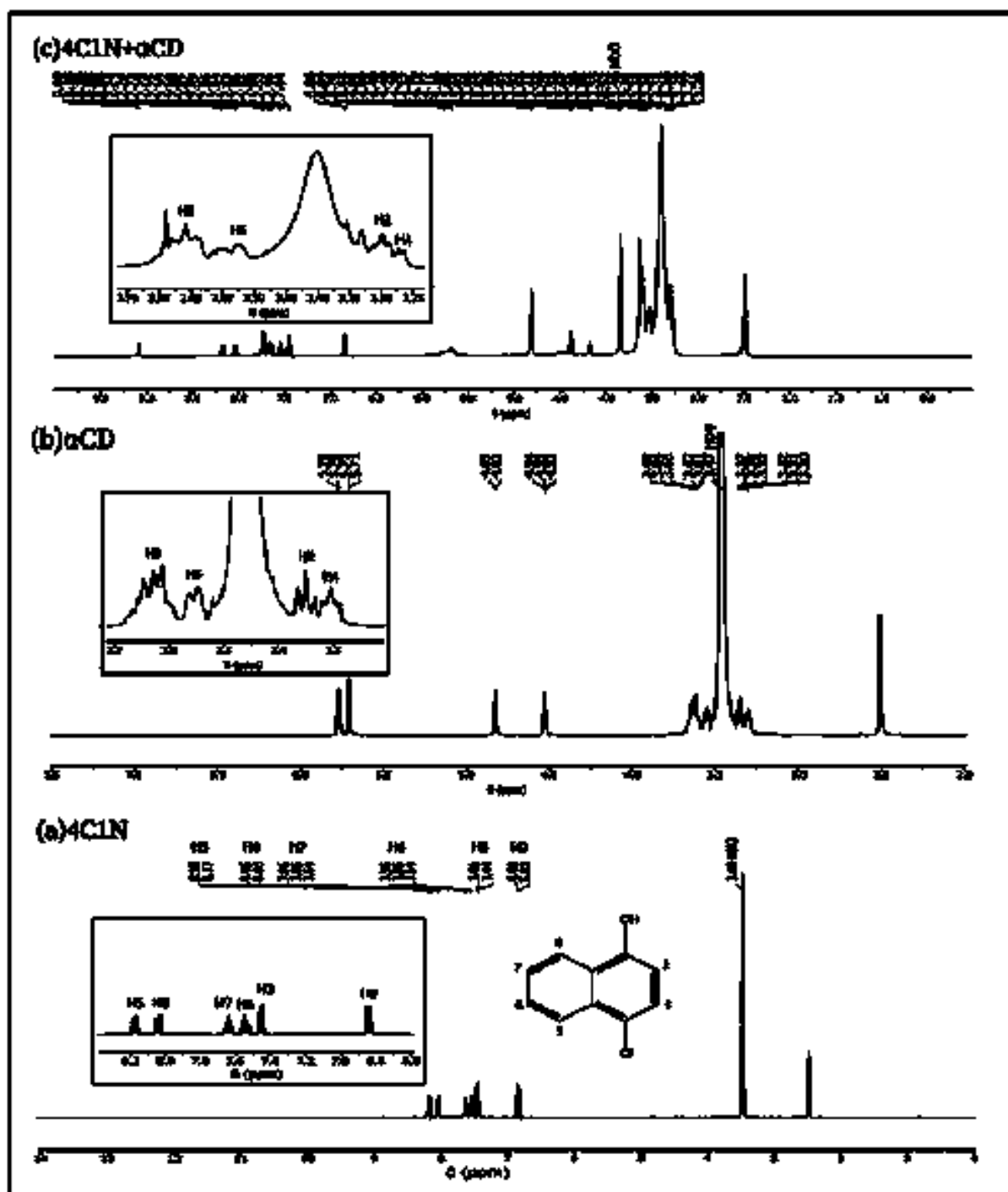
- **Figure VII.1.** Variations in the surface tension ( $\gamma$ ) of 4C1N in aqueous ethanol with increasing concentration of  $\alpha$ -CD and  $\beta$ -CD at 298.15K

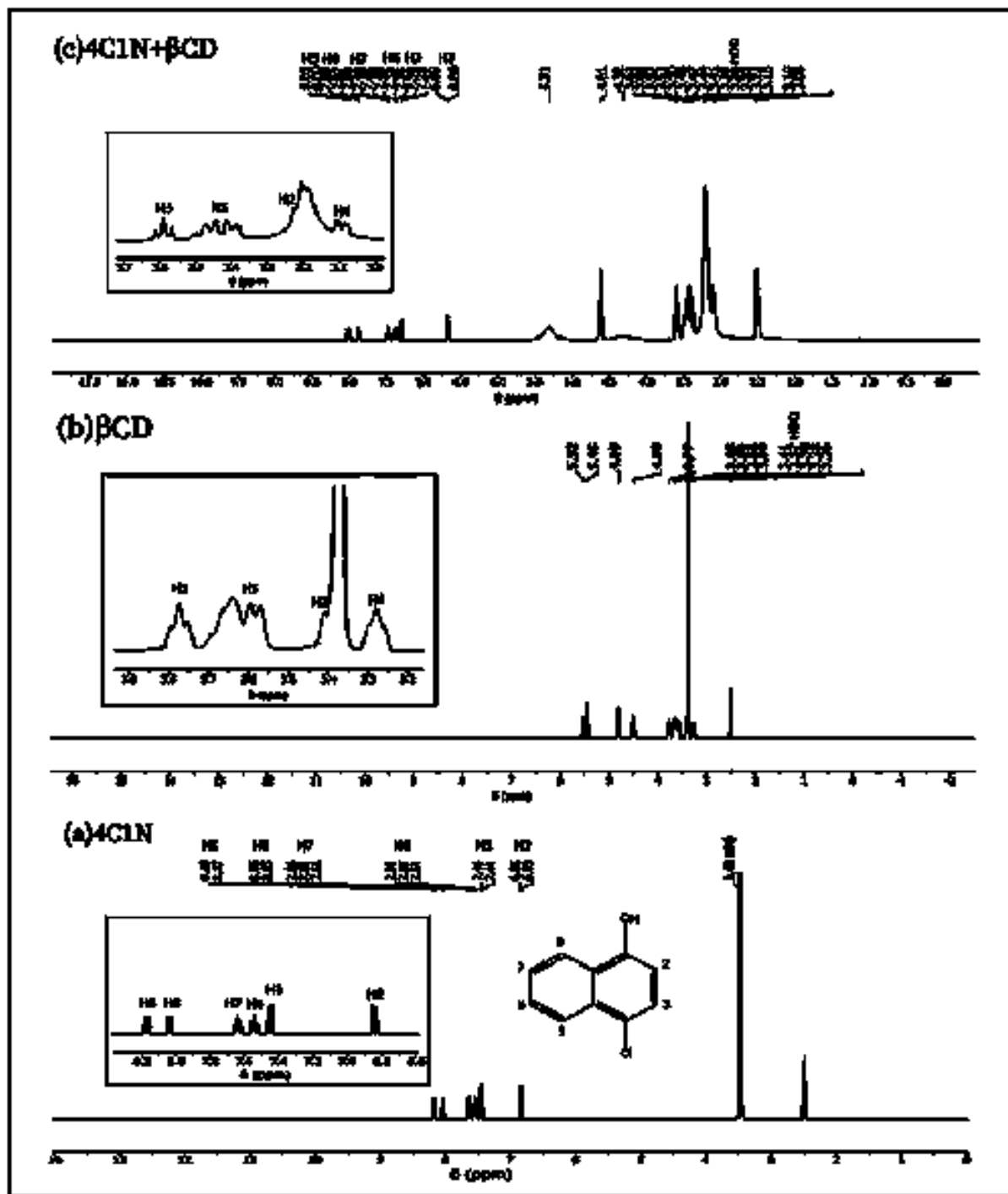


- **Figure VII.2.** Job plots of (a) [4C1N+ $\alpha$ -CD] (red) and (b) [4C1N+ $\beta$ -CD](orange)



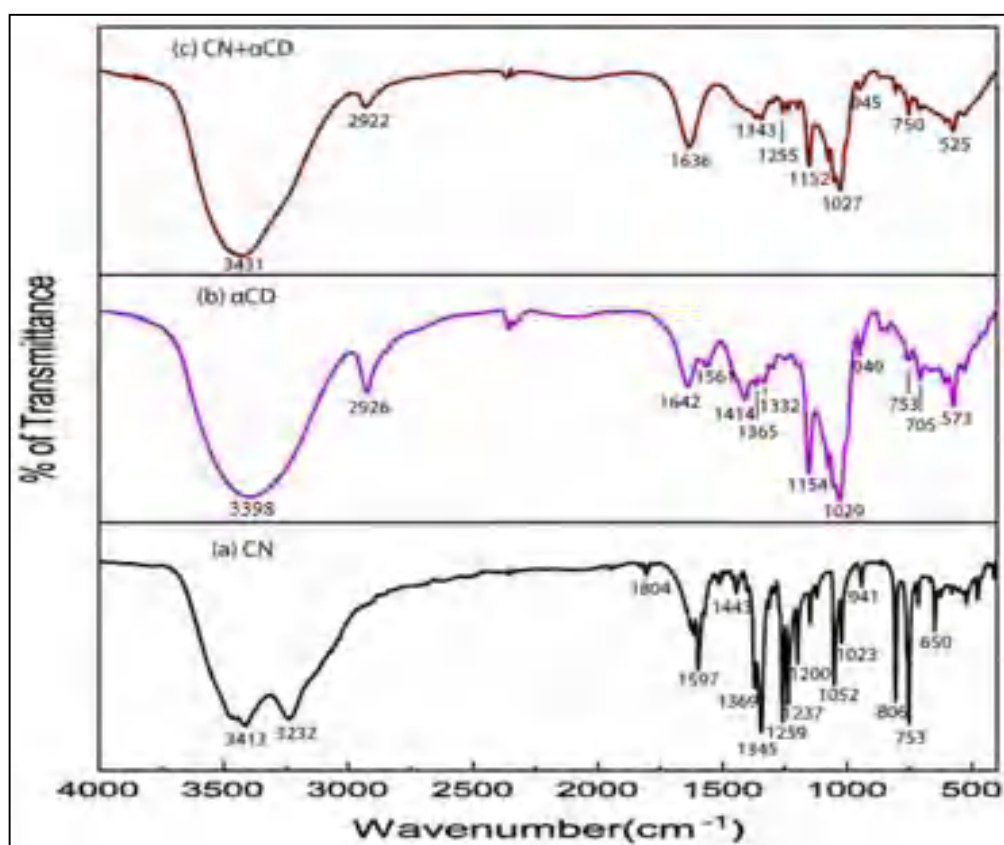
■ Figure VII.3.  $^1\text{H}$  NMR spectra of IC1,  $\alpha$ -CD and 4C1N at 298.15 K



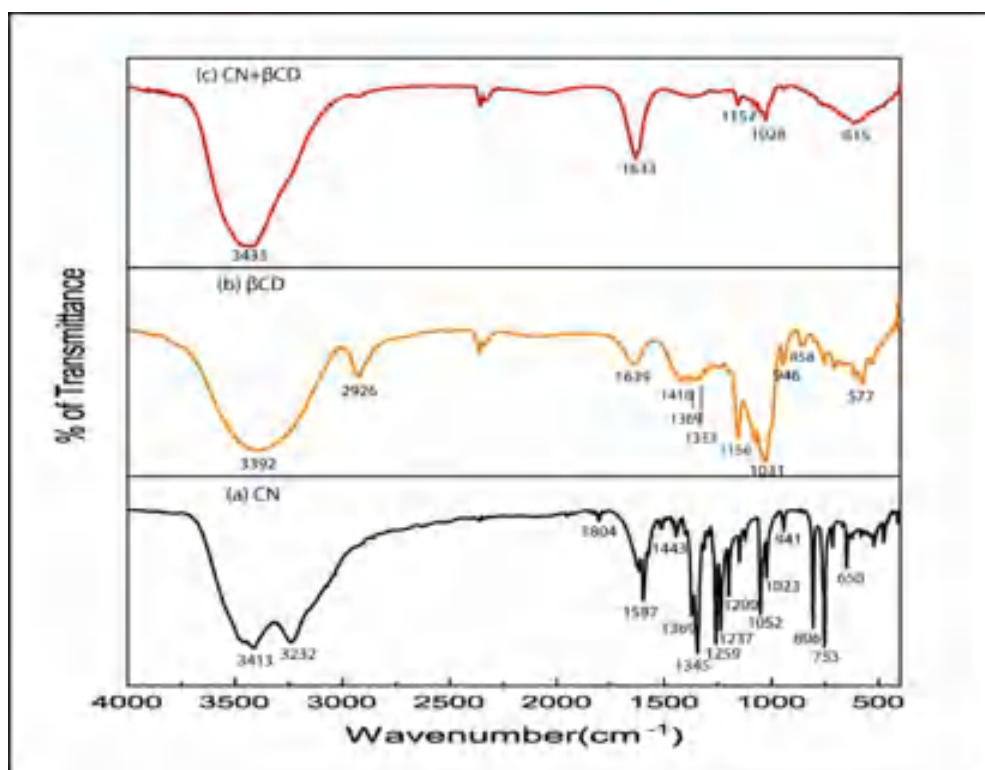
■ Figure VII.4.  $^1\text{H}$  NMR spectra of IC2,  $\beta$ -CD and 4C1N at 298.15K



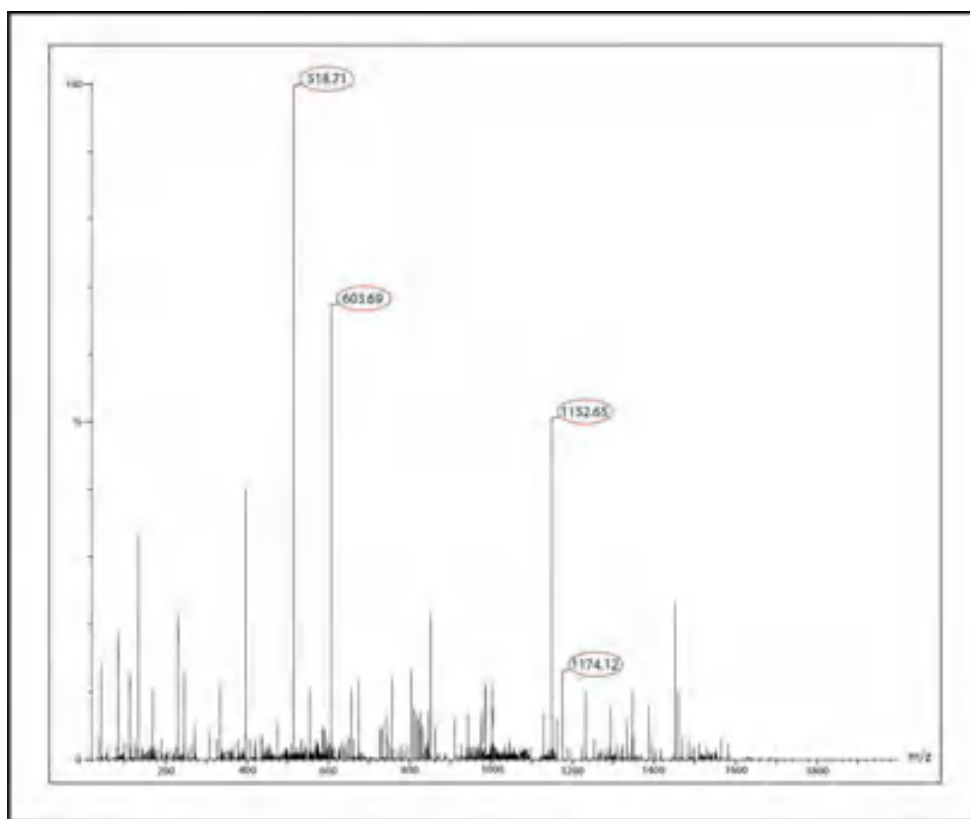
■ **Figure VII.5.** FT-IR spectra of 4C1N,  $\alpha$ -CD and the solid complex (IC1)



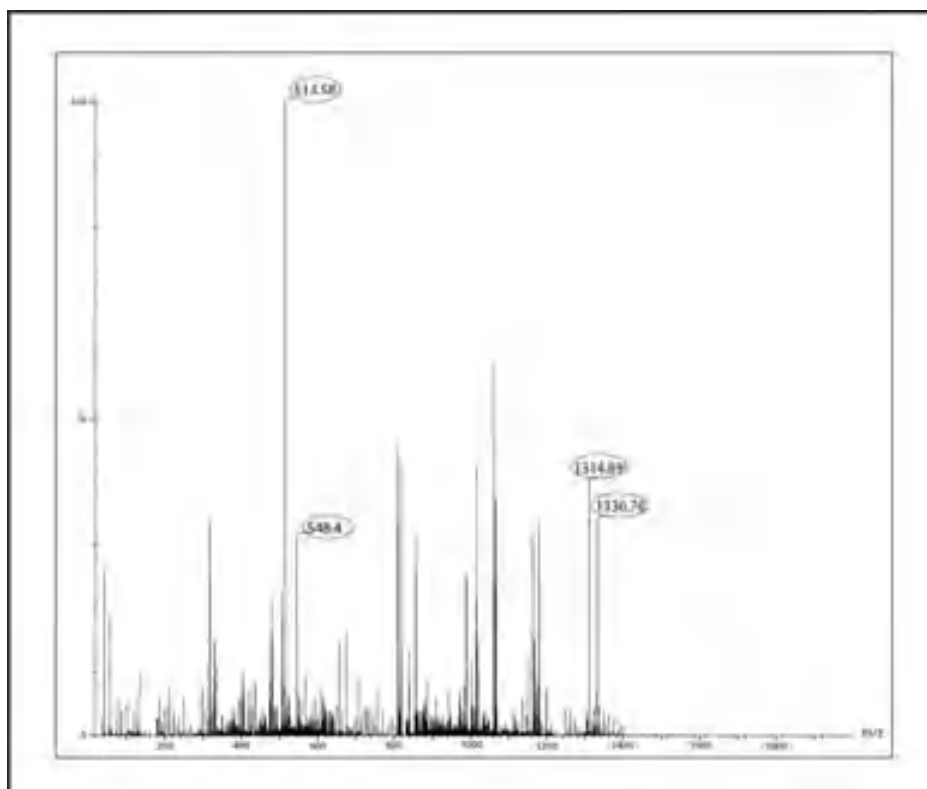
■ **Figure VII.6.** FT-IR spectra of 4C1N,  $\beta$ -CD and the solid complex (IC2)



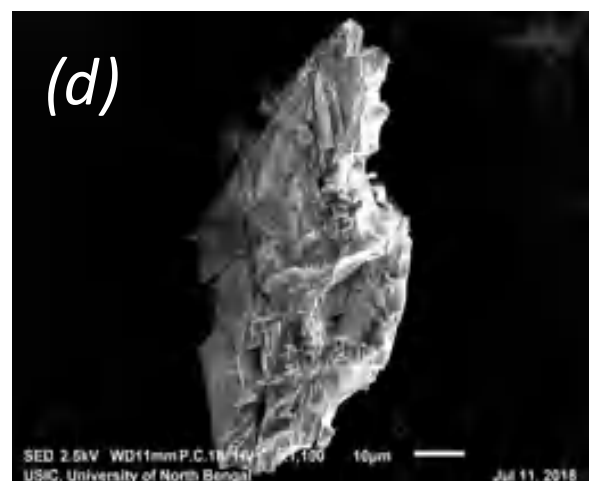
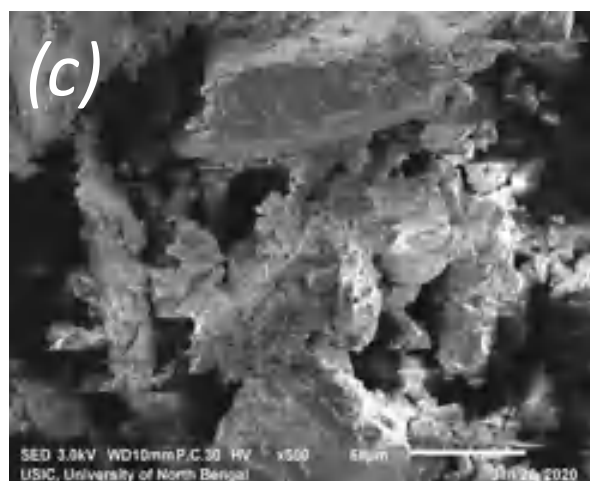
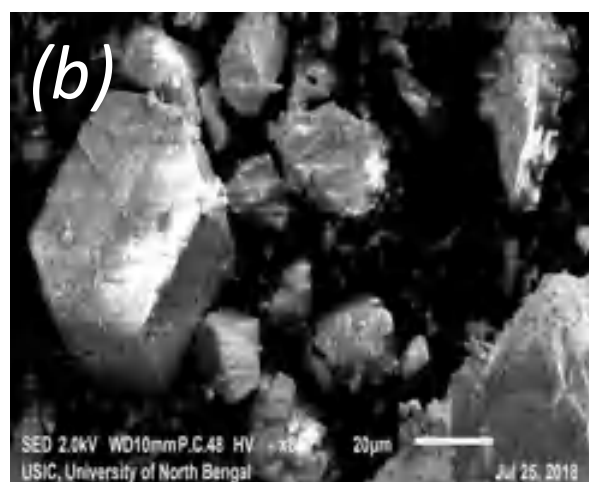
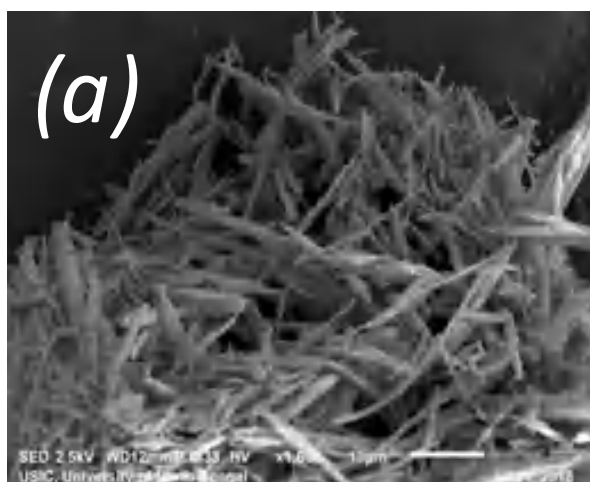
■ **Figure VII.7.** HRMS of (4C1N+ $\alpha$ -CD) inclusion complex



■ **Figure VII.8.** HRMS of (4C1N+ $\beta$ -CD) inclusion complex

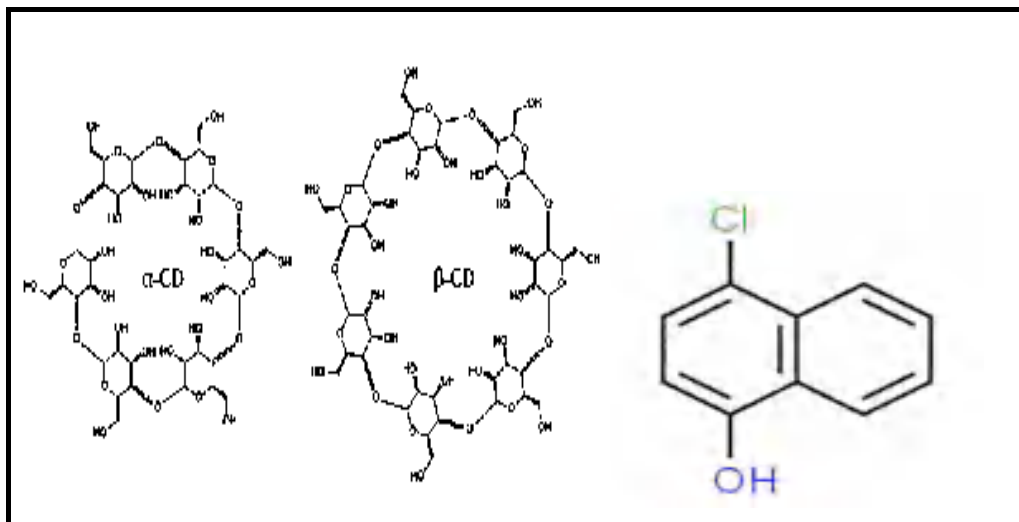


■ **Figure VII.9.** Scanning electron photograph for (a) 4C1N (b)  $\alpha$ -CD (c)  $\beta$ -CD (d) 4C1N+ $\alpha$ -CD and (e) 4C1N+ $\beta$ -CD

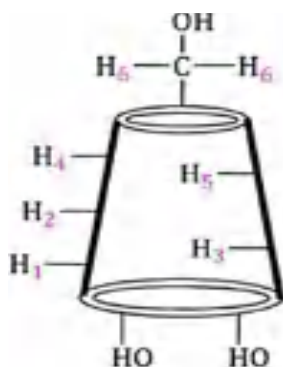


**SCHEMES**

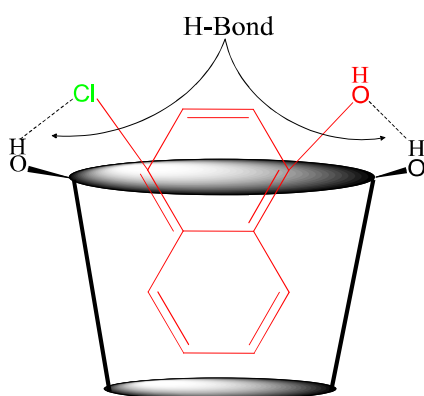
- **Scheme VII.1.** molecular structure of  $\alpha$ -CD,  $\beta$ -CD and 4-chloro-1-naphthol



- **Scheme VII.2.** Various hydrogen atoms in cyclodextrin molecule



- **Scheme VII.3.** 4-chloro-1-naphthol+Cyclodextrin 1:1 inclusion complex



## SUPPORTING DATA

■ **Table S1.** Association constant data of 4C1N+  $\alpha$ -CD in different temperatures

Temp /K	[4C1N] / $\mu$ M	[ $\alpha$ -CD] / $\mu$ M	$A_0 \times 10^2$	$A \times 10^2$	$\Delta A \times 10^2$	$1/[\alpha\text{-CD}] \times 10^{-3} / \text{M}^{-1}$	$1/\Delta A$	Intercept	Slope $\times 10^4$	$K_a / \text{M}^{-1}$
293.15	50	30	240.37	243.18	2.80	33.33	35.62			
	50	40	240.37	243.88	3.50	25.00	28.55			
	50	50	240.37	244.68	4.31	20.00	23.19	5.40	9.11	5930.74
	50	60	240.37	245.13	4.76	16.67	21.00			
	50	70	240.37	245.88	5.50	14.29	18.17			
298.15	50	30	231.77	234.59	2.81	33.33	35.47			
	50	40	231.77	235.26	3.48	25.00	28.66			
	50	50	231.77	236.15	4.37	20.00	22.83	4.03	9.54	4227.01
	50	60	231.77	236.75	4.97	16.67	20.11			
	50	70	231.77	237.53	5.75	14.29	17.38			
303.15	50	30	219.88	222.07	2.19	33.33	45.69			
	50	40	219.88	222.60	2.72	25.00	36.75			
	50	50	219.88	223.15	3.27	20.00	30.56	3.13	13.10	2399.99
	50	60	219.88	223.88	4.00	16.67	24.98			
	50	70	219.88	224.79	4.91	14.29	20.36			

■ **Table S2.** Association constant data of 4C1N+  $\beta$ -CD in different temperatures

Temp /K	[4C1N] / $\mu$ M	[ $\beta$ -CD] / $\mu$ M	$A_0 \times 10^2$	$A \times 10^2$	$\Delta A \times 10^2$	$1/[\beta\text{-CD}] \times 10^{-3} / \text{M}^{-1}$	$1/\Delta A$	Intercept	Slope $\times 10^4$	$K_a / \text{M}^{-1}$
293.15	50	30	240.38	243.17	2.79	33.33	35.88			
	50	40	240.38	243.55	3.17	25.00	31.52			
	50	50	240.38	244.23	3.85	20.00	25.95	6.42	9.24	6950.53
	50	60	240.38	245.07	4.66	16.67	21.47			
	50	70	240.38	245.82	5.44	14.29	18.38			
298.15	50	30	231.78	234.30	2.52	33.33	39.70			
	50	40	231.78	234.84	3.06	25.00	32.70			
	50	50	231.78	235.38	3.57	20.00	28.02	5.20	10.60	4902.76
	50	60	231.78	236.16	4.39	16.67	22.79			
	50	70	231.78	237.03	5.25	14.29	19.04			
303.15	50	30	219.88	221.77	1.89	33.33	52.95			
	50	40	219.88	222.30	2.42	25.00	41.30			
	50	50	219.88	222.75	2.87	20.00	34.81	4.48	14.70	3047.21
	50	60	219.88	223.38	3.50	16.67	28.54			
	50	70	219.88	223.89	4.01	14.29	24.92			